

# Constraints on large- $x$ parton distributions from new weak boson production and deep-inelastic scattering data

A. Accardi<sup>1,2</sup>, L. T. Brady<sup>2,3</sup>, P. J. Ehlers<sup>2,4</sup>, C. E. Keppel<sup>2</sup>,

W. Melnitchouk<sup>2</sup> J. F. Owens<sup>5</sup>, Nobuo Sato<sup>2</sup>, ...

<sup>1</sup>*Hampton University, Hampton, Virginia 23668*

<sup>2</sup>*Jefferson Lab, Newport News, Virginia 23606*

<sup>3</sup>*University of California, Santa Barbara, California 93106, USA*

<sup>4</sup>*University of Washington, Seattle, Washington 98195, USA*

<sup>5</sup>*Florida State University, Tallahassee, Florida 32306, USA*

**CTEQ-Jefferson Lab (CJ) Collaboration**

(Dated: August 16, 2015)

## Abstract

We present a new set of leading twist parton distribution functions (PDFs), which take advantage of developments in the theoretical treatment of nuclear corrections as well as new data. The analysis includes for the first time data on the free neutron structure function from the BONuS experiment at Jefferson Lab, and new charged lepton and  $W$ -boson asymmetry data from Fermilab, which significantly reduce the uncertainty on the  $d/u$  ratio at large values of  $x$ .

## I. INTRODUCTION

... general intro ...

... what is new since CJ12 ...

• more complete/consistent/systematic treatment of nuclear corrections esp. nucleon off-shell corrections

• impact of new  $W$ -boson asymmetry data on  $d/u$  ratio

• inclusion of JLab (BONuS) data

• analysis of  $\bar{d} - \bar{u}$  at large  $x$  ... choose either  $\bar{d}/\bar{u} \rightarrow 1$  or  $0$  as  $x \rightarrow 1$  ...

• S-ACOT scheme for heavy quarks

• LO fit

•  $\alpha_s$  treatment

... In Sec. II we ...

## II. THEORETICAL FOUNDATIONS

In this section we present the theoretical framework that is used for the CJ15 analysis.

### A. PDF parametrizations

...[OLD TEXT]...

For the parametrization of the PDFs at the input scale  $Q_0^2$ , a common form has been adopted for all parton species  $f$ ,

$$xf(x, Q_0^2) = a_0 x^{a_1} (1-x)^{a_2} (1 + a_3 \sqrt{x} + a_4 x). \quad (1)$$

This form applies to the valence distributions  $xq_v \equiv x(q - \bar{q})$ , for  $q = u$  and  $d$ , the isoscalar and isovector sea quark distributions  $x(\bar{u} + \bar{d})$  and  $x(\bar{d} - \bar{u})$ , and the gluon distribution  $xg$ . However, to allow for a more flexible parametrization of the valence  $d_v$  PDF in the large- $x$  region, we add in a small admixture of the  $u_v$  PDF,

$$d_v \rightarrow a_0^{d_v} \left( \frac{d_v}{a_0^{d_v}} + b x^c u_v \right), \quad (2)$$

with  $b$  and  $c$  as two additional parameters. The result of this modification is that  $d_v/u_v \rightarrow a_0^{d_v} b$  as  $x \rightarrow 1$ , provided  $a_2^{d_v} > a_2^{u_v}$ , which is usually the case. A finite, nonzero value of this

ratio is indeed expected in several nonperturbative models of hadron structure [6–8]. It is also required from a purely practical point of view, as it avoids potentially large biases on the  $d$ -quark PDF central value [14], as well as on its PDF error estimate, as we discuss in detail in Sec. IV. The  $a_0$  parameters for the  $u_v$  and  $d_v$  distributions are fixed by the appropriate valence quark number sum rules, while  $a_0^g$  is fixed by the momentum sum rule.

- New parametrization for  $\bar{d} - \bar{u}$  ... avoids negative PDFs? ...

In our analysis we parametrize the  $\bar{d}/\bar{u}$  ratio as

$$\frac{\bar{d}}{\bar{u}} = a_0 x^{a_1} (1-x)^{a_2} + 1 + x^{a_3} (1-x)^{a_4}, \quad (3)$$

which ensures that in the limit  $x \rightarrow 1$  one has  $\bar{d}/\bar{u} \rightarrow 1$ . The existing data are not able to reliably determine the large- $x$  behavior of the ratio, so as an alternative we also perform fits using  $\bar{d}/\bar{u} = a_0 x^{a_1} (1-x)^{a_2} + (1+x^{a_3})(1-x)^{a_4}$ , which vanishes in the  $x \rightarrow 1$  limit. The  $\bar{d}/\bar{u} \rightarrow 1$  limit is what would be expected from perturbative QCD, while the  $\bar{d}/\bar{u} \rightarrow 0$  limit may arise if the trend in  $x \gtrsim 0.3$  points from the E866 experiment [28] were to continue to larger  $x$ .

## B. Heavy quarks

- Implementation of S-ACOT scheme.

## C. $1/Q^2$ corrections

- For target mass corrections, use of OPE (G-P); ... comparisons with EFP, series expansion; ... in practice doesn't matter! (?)
- For other subleading  $1/Q^2$  corrections, such as higher twist and other residual power corrections (
- ... anything different to CJ12??

$$F_2(x, Q^2) = F_2^{\text{LT}}(x, Q^2) \left( 1 + \frac{C(x)}{Q^2} \right), \quad (4)$$

where  $F_2^{\text{LT}}$  denotes the leading twist structure function including TMCs. For simplicity we generically refer to the fitted  $1/Q^2$  term as a “higher twist” correction, and parametrize the

higher twist coefficient function by  $C(x) = a_{\text{HT}} x^{b_{\text{HT}}}(1 + c_{\text{HT}}x)$ , assuming it to be isospin independent (see, however, Refs. [60–63]).

#### D. Nuclear corrections

- The analysis includes nuclear corrections for deuterium account for nucleon Fermi motion and nuclear binding effects, which are implemented using nuclear smearing functions, as well as rescattering effects mediated by Pomeron and meson exchange mechanisms which give rise to shadowing at small  $x \lesssim 0.1$  and a small amount of antishadowing at  $x \sim 0.1$ . For the shadowing and antishadowing corrections, the model of Ref. [1] is used (see also Refs. [2, 3]), although the effects of these is negligible in our analysis.

The implementation of the nuclear smearing

##### 1. Nuclear smearing

Since nucleons bound in a nucleus are not free, the nuclear structure function deviates from a simple sum of free proton and neutron structure functions, especially at large  $x$  where the effects of Fermi motion, nuclear binding, and nucleon off-shellness are most prominent. In the nuclear impulse approximation the structure function of the deuteron  $d$  can be expressed as a generalized convolution of the bound nucleon structure function and a momentum distribution  $f_{N/d}$  of nucleons in the deuteron [64, 65],

$$q^d(x, Q^2) = \int \frac{dz}{z} dp^2 f_{N/d}(z, p^2) \tilde{q}^N(x/z, p^2, Q^2), \quad (5)$$

where  $f_{N/d}(z, p^2)$  gives the (light-cone) distribution of nucleons in the deuteron for a given nucleon momentum fraction in the deuteron  $z = (M_d/M)(p \cdot q / p_d \cdot q)$  and nucleon virtuality  $p^2$ , where  $p$  and  $p_d$  are the four-momenta of the nucleon and deuteron, respectively, and  $M_d$  is the deuteron mass. The function  $\tilde{q}^N$  is the off-shell nucleon structure function, and a sum over the nucleons  $N = p, n$  is implied. ... The function  $\tilde{q}^N$  includes  $1/Q^2$  corrections, such as TMCs and higher twist effects. ... Expanding the off-shell nucleon structure function about the on-shell limit, one finds [66]

$$\tilde{q}^N(x, p^2, Q^2) = q^N(x, Q^2) \left( 1 + \frac{p^2 - M^2}{M^2} \delta f^N(x, Q^2) \right), \quad (6)$$

where the coefficient of the off-shell term is

$$\delta f^N(x, Q^2) = \left. \frac{\partial \ln \tilde{q}^N(x, p^2, Q^2)}{\partial \ln p^2} \right|_{p^2=M^2}, \quad (7)$$

and the  $\tilde{q}^N$  includes the parametrized higher twist corrections of Eq. (4). The on-shell term leads to the standard on-shell convolution representation for the nuclear structure function, while the off-shell term can be evaluated as an additive correction,  $q^d = q^{d(\text{on})} + q^{d(\text{off})}$ , where

$$q^{d(\text{on})}(x, Q^2) = \int \frac{dz}{z} f^{(\text{on})}(z) q^N(x/z, Q^2), \quad (8a)$$

$$q^{d(\text{off})}(x, Q^2) = \int \frac{dz}{z} f^{(\text{off})}(z) \delta f^N(x/z, Q^2) q^N(x/z, Q^2). \quad (8b)$$

The on-shell and off-shell smearing functions  $f^{(\text{on})}$  and  $f^{(\text{off})}$  are taken to be the same for the proton and neutron, and are given by [68]

$$f^{(\text{on})}(z) = \int dp^2 f_{N/d}(z, p^2), \quad (9a)$$

$$f^{(\text{off})}(z) = \int dp^2 \frac{p^2 - M^2}{M^2} f_{N/d}(z, p^2). \quad (9b)$$

The momentum distributions, or “smearing functions”,  $f^{(\text{on})}$  and  $f^{(\text{off})}$ , are computed in the weak binding approximation (WBA) in terms of the deuteron wave function, and include the effects of nuclear binding and Fermi motion [66, 67]. At  $Q^2 \rightarrow \infty$  the on-shell smearing function  $f^{(\text{on})}$  has a simple probabilistic interpretation in terms of the light-cone momentum fraction  $z \approx (M_d/M)(p^+/p_d^+)$  of the deuteron carried by the struck nucleon, while at finite  $Q^2$  it depends in addition on the parameter  $\rho^2 = 1 + 4x^2 M^2/Q^2$ , which characterizes the deviation from the Bjorken limit.

The nuclear corrections at large  $x$  depend partly on the strength of the high-momentum tail of the deuteron wave function, and we use several wave functions based on different nucleon–nucleon potentials to study the deuteron model dependence. We choose the high-precision AV18 [69], CD-Bonn [70] and the relativistic WJC-1 and WJC-2 [71] wave functions, which provide a representative spread of behaviors at high momentum. Note that the effects of the nuclear smearing corrections are not suppressed at large  $Q^2$ , and must be considered at all scales wherever data at  $x \gtrsim 0.3$  are used [11–13].

- Same off-shell functions in DIS and DY.

## 2. Nucleon off-shell corrections

- The off-shell nucleon correction  $\delta^{(\text{off})}q^d$  is somewhat more model dependent, but several quark model based estimates of this have been made in the literature [66, 72, 73].

- ... give brief history of off-shell corrections

- MST (theoretical)

- KP (model/fitted)

- CJ11 (mKP)

- CJ12 (more consistent mKP)

- CJ15 (calculation at parton level - different treatment of valence quarks, antiquarks and gluons - can apply to any observable, not just  $F_2$  structure function - in CJ11 and CJ12 had used overall multiplicative constant, only for  $F_2$ )

- In Ref. [14] this was computed using the “modified Kulagin-Petti” model. In this model, the corrections were related to the change in the nucleon’s confinement radius in the nuclear medium, as well as the average virtuality of the bound nucleons, and constrained to give no net change in the structure function normalization. In contrast to Ref. [14], however, here we further take into account the correlation between the nucleon “swelling” and the deuteron wave function. The combined effects introduce a theoretical uncertainty in the extracted PDFs, particularly for the  $d$  quark.

- In CJ15 have freed off-shell parameters, allowing them to be determined by the fit. Using either fmKP model (rescaling parameter  $\lambda$ ), or in phenomenological fit.

- In this analysis, we explore the possibility of antishadowing in the deuteron, suggested in the global nuclear analysis of KP [66], in which the  $F_2^d/F_2^N$  ratio is slightly enhanced (above unity) at  $x \approx 0.1 - 0.2$ . To allow for one or more zero crossings in the function  $\delta f^N$ , we use the same parametrization as in Ref. [66],

$$\delta f^N = C_N(x - x_0)(x - x_1)(x - x_2), \quad (10)$$

but fit the parameters to the deuterium data. The requirement that the off-shell correction does not modify the number of valence quarks in the nucleon provides the constraint

$$\int_0^1 dx \delta f^N(x) (q(x) - \bar{q}(x)) = 0. \quad (11)$$

## E. PDF Errors

... as for CJ12 ... Hessian ... tolerance ...

## III. DATA

The CJ15 PDFs are obtained by fitting to a global database of 4035 data points from a variety of high energy scattering processes, listed in Table I. These include deep-inelastic scattering data from BCDMS, NMC, SLAC, HERA and Jefferson Lab; Drell-Yan  $p$  and  $d$  cross sections from fixed target experiments at Fermilab;  $W$  and  $Z$  asymmetries, as well as jet and  $\gamma$ +jet cross sections from the CDF and DØ collaborations at the Tevatron. The table also lists the corresponding  $\chi^2$  values for each data set. The overall  $\chi^2/\text{dof}$  is 0.98. The fit is slightly better than in our previous CJ12 analysis [15], partly because of the greater flexibility which we have allowed in the current fit for the nucleon off-shell corrections.

The quality of the fit to the data is illustrated in Fig. 1, where a subset of the world's proton  $F_2^p$  structure function data (from BCDMS, NMC, SLAC and Jefferson Lab) is shown over several decades of  $Q^2$  for various fixed values of  $x$ . Cuts on the kinematical coverage of the data have been made for  $Q^2 > 1.69 \text{ GeV}^2$  and  $W^2 > 3.5 \text{ GeV}^2$ .

\* JLab data are at varying  $x$  and  $Q^2$  values

\* Similar agreement for  $F_2^d$

\* Show HERA data separately??

## IV. RESULTS

In this section we present the results of the global analysis for the CJ15 PDFs. After discussing the general features of the distributions, we focus our attention on the effects of nuclear corrections on the PDFs, and particular the ratio of  $d$ - to  $u$ -quark distributions.

### A. CJ15 PDFs

The CJ15 PDFs are displayed in Fig. 2 as a function of  $x$  at a scale of  $Q^2 = 10 \text{ GeV}^2$ , for the  $u$ ,  $d$ ,  $\bar{d} + \bar{u}$  and  $\bar{d} - \bar{u}$  distributions, and the gluon distribution scaled by a factor 1/10. The central CJ15 PDFs are determined using the AV18 deuteron wave function and

TABLE I: Data sets used in the CJ15 global analysis, with the corresponding number of data points and the respective  $\chi^2$  values for each set.

	experiment	# points	$\chi^2$
DIS $F_2$	BCDMS ( $p$ ) [22]	351	437
	BCDMS ( $d$ ) [22]	254	294
	NMC ( $p$ ) [23]	275	407
	NMC ( $d/p$ ) [24]	189	172
	SLAC ( $p$ ) [25]	564	435
	SLAC ( $d$ ) [25]	582	372
	JLab ( $p$ ) [26]	136	166
	JLab ( $d$ ) [26]	136	124
	JLab ( $n/d$ ) [83]	191	217
DIS $\sigma$	HERA (NC $e^-$ ) [27]	145	112
	HERA (NC $e^+$ ) [27]	408	541
	HERA (CC $e^-$ ) [27]	34	19
	HERA (CC $e^+$ ) [27]	34	31
Drell-Yan	E605 ( $pCu/N??$ ) [44]	119	9
	E866 ( $pp$ ) [28]	121	139
	E866 ( $pd$ ) [28]	129	144
	E866 ( $pd/pp$ ) [29]	12	9
$W$ /lepton asymmetry	CDF ( $e$ ) [30]	11	12
	DØ ( $\mu$ ) [31]	10	20
	DØ ( $e$ ) [32]	13	27
	CDF ( $W$ ) [33]	13	15
	DØ ( $W$ ) [34]	14	16
$Z$ rapidity	CDF ( $Z$ ) [35]	28	27
	DØ ( $Z$ ) [36]	28	16
jet	CDF (run 2) [38]	72	15
	DØ (run 2) [40]	110	21
$\gamma$ +jet	DØ 1 [41]	16	6
	DØ 2 [41]	16	15
	DØ 3 [41]	12	25
	DØ 4 [41]	12	13
Total		4035	3941
Total + norm			3950
$\chi^2/\text{dof}$			0.979

the nucleon off-shell parametrization in Eq. (10). These are compared with PDFs from several other global parametrizations ... and their uncertainties, in the form of ratios to the central CJ15 distributions. Since different PDF analyses typically utilize different criteria for estimating the PDF errors, we display the CJ15 errors for the standard  $\Delta\chi^2 = 1$ , or



tolerance  $T = 1$ , as well as with errors inflated by a tolerance of  $T = 10$ . HERAPDF15 for instance uses  $\Delta\chi^2 = 1$ , while the recent MMHT14 analysis uses a ... .. method.

- \* uncertainty on  $d$  much larger at high  $x$  than on  $u$

- \* since HERAPDF15 uses only HERA data on inclusive cross sections, these PDFs are not well constrained at high  $x$ ;  $\bar{d} - \bar{u}$  is not constrained.

- \* MMHT14 uncertainties are typical of other modern global fits, such as CT14 [18] or NNPDF3.0 [19].

- \* other features worth discussing?

## B. PDFs at large $x$

The effects of nuclear corrections on the PDFs are illustrated in Fig. 6, where several different deuteron wave function models have been used in the fits. The distributions are displayed relative to the central CJ15 PDFs which use the AV18 deuteron wave function. The results using the CD-Bonn or WJC-2 wave function are very similar to those for the AV18 wave function, while using the WJC-1 model leads to larger differences. This suggests that, for the most part, the nucleon off-shell parametrization in Eq. (10) is sufficiently flexible so as to be able compensate for changes induced by the different wave functions. For the WJC-1 wave function, which has the hardest momentum distribution, it is more difficult for the off-shell correction to compensate. Recall from Table I that the AV18, CD-Bonn and WJC-2 models give the lowest values of  $\chi^2/\text{dof}$  (...), while the WJC-1 model gives the largest value.

As expected, the variations due to the nuclear models have the largest effects in the  $d$ -quark distribution, which is less constrained by proton data and hence more sensitive to uncertainties in the extracted neutron structure function. The spread in the  $d$  PDF at  $x = 0.8$  is  $\approx 20\%$  for the various wave functions. The variations for the AV18, CD-Bonn and WJC-2 wave functions are generally within the  $\Delta\chi^2 = 1$  confidence limit, while the WJC-1 results lie outside the band for the  $u$  and  $d$  PDFs. Interestingly, one observes an anti-correlation between the behavior of the  $d$ -quark distribution at large  $x$  and the gluon distribution. In fact, using the WJC-1 wave functions leads to slight decreases in all the quark PDFs at high  $x$ , while the gluon PDF has the opposite trend. The spread in the gluon PDF is  $\lesssim 10\%$  for  $x < 0.8$ , although beyond  $x \approx 0.3$  the gluon distribution has a very large

uncertainty.

Using the 1-parameter off-shell rescaling model (ORM) for the nucleon off-shell corrections, the corresponding PDF ratios are displayed in Fig. 7. For the AV18, CD-Bonn and WJC-2 wave functions, the effects of using the more flexible off-shell parametrization (10) and the more restrictive ORM form are very small, and generally within the  $\Delta\chi^2 = 1$  bands. For the WJC-1 wave function, the results for the  $d$ -quark PDF show significantly greater deviation at large  $x$ , again suggesting that the off-shell rescaling model is not able to compensate for the hard tail of its momentum distribution. In addition, for the  $u$ -quark distribution the WJC-1 result lies slightly outside the uncertainty band at  $x \sim 0.05$ .

### C. $d/u$ ratio

The impact of the nuclear corrections and data constraints on the  $d/u$  ratio are illustrated in Figs. 11 and 12.

In Fig. 11:

- BONuS data shrink error on  $d/u$  slightly in the  $x \approx 0.5 - 0.6$  range
- significant reduction in error once  $W$  asymmetry data added
- For other deuteron wave function models, the total  $\chi^2$  values are very similar, with  $\chi^2/\text{dof} = 0.979$  for the CD-Bonn wave function, 0.983 for the WJC-1 wave function, and 0.980 for the WJC-2 model. The AV18, CD-Bonn and WJC-2 model fits are therefore essentially indistinguishable, while the WJC-1 model, with its significantly harder deuteron wave function, has a slightly worse overall fit.

• With the off-shell covariant spectator (OCS) model ...[WHAT WE HAD BEEN CALLING “fmKP”]..., the  $\chi^2$  values for the various wave functions are marginally higher, with  $\chi^2/\text{dof} = 0.982, 0.982, 0.989$  and 0.984 for the AV18, CD-Bonn, WJC-1 and WJC-2 models. Here again the WJC-1 gives the worst fit. ...[MORE DISCUSSION]...

- impact of various data sets on  $d/u$  ratio:
  - DIS only: large uncertainty
  - BONuS shrinks uncertainty appreciably at  $x \sim 0.6$
  - lepton asymmetry data gives significant reduction in uncertainty at  $0.2 \lesssim x \lesssim 0.4$ , with smaller reduction at larger  $x$
  - $Z$  rapidity data, on the other hand, has very little effect on the uncertainty

- $W$  asymmetry data, in particular the DØ data [34], gives significant reduction in the  $d/u$  uncertainty for  $x \gtrsim 0.6$

The effects of deuterium data and the nuclear corrections in the deuterium data are illustrated in Fig. 12:

- with no nuclear corrections the  $d/u$  ratio is larger at  $x \gtrsim 0.6$  than with the nuclear corrections. This can be understood from the shape of the  $F_2^d/F_2^N$  ratio Fig. 5 at large  $x$ , where the effect of the nuclear corrections is to increase the ratio above unity for  $x \gtrsim 0.6$ . Since  $F_2^d$  and  $F_2^p$  are fixed inputs, a larger  $F_2^d/F_2^N$  is generated by a smaller neutron  $F_2^n$  and hence a smaller  $d/u$  ratio. For example, the effect of the nuclear corrections is to shift the  $d/u$  ratio at  $x = 0.8$  from the ( $T = 10$ ) range  $\approx 0.1 - 0.3$  to  $\approx 0 - 0.2$  once the smearing and off-shell effects are included.

- removing the deuterium data altogether increases the overall uncertainty band for  $x \gtrsim 0.7$ . Interestingly, the deuteron data also reduce the  $d/u$  uncertainties slightly at smaller  $x$ ,  $x \lesssim 0.1$ .

The final CJ15  $d/u$  results and uncertainties (for  $T = 10$ ) can be compared with ratios obtained in other recent global PDF analyses. These are shown in Fig. 10 for the MMHT14 [17], CT14 [18] and JR14 [47] PDFs.

- JR14 uses similar experimental data sets and treatment of nuclear and finite- $Q^2$  corrections at large  $x$ ;
- JR14 has largest uncertainty in the intermediate- $x$  region, which may result from the recent  $W$  and lepton asymmetry data from CDF and DØ not being used;
- at large  $x$  the JR14  $d/u$  ratio  $\rightarrow 0$  from the form of their parametrization;
- CT14 range is similar

#### D. $\bar{d} - \bar{u}$ asymmetry ...[SAVE FOR LATER PAPER??]...

... Connection with Gottfried sum ... Peng et al. paper ...

## V. CONCLUSION

### Acknowledgments

We thank E. Christy, P. Monaghan, ... for helpful discussions. This work was supported by the DOE contract No. DE-AC05-06OR23177, under which Jefferson Science Associates, LLC operates Jefferson Lab. The work of J.F.O. and A.A. was supported in part by DOE contracts No. DE-FG02-97ER41922 and No. DE-SC0008791, respectively.

## Appendix A: Parameter values

In this appendix we list the initial parameter values and their errors for the CJ15 PDFs, for the leading twist, off-shell and higher twist parameters, as discussed in the text. The parameters without errors have been fixed by sum rules or other constraints.

- 
- [1] W. Melnitchouk and A. W. Thomas Phys. Rev. D **47**, 3783 (1993).
  - [2] B. Badelek and J. Kwiecinski, Nucl. Phys. **B370**, 278 (1992).
  - [3] L. P. Kaptari and A. Yu. Umnikov, Phys. Lett. B **272**, 359 (1991).
  - [4] R. P. Feynman, *Photon Hadron Interactions* (Benjamin, Reading, Massachusetts, 1972).
  - [5] F. E. Close, Phys. Lett. B **43**, 422 (1973).
  - [6] G. R. Farrar and D. R. Jackson, Phys. Rev. Lett. **35**, 1416 (1975).
  - [7] W. Melnitchouk and A. W. Thomas, Phys. Lett. B **377**, 11 (1996).
  - [8] R. J. Holt and C. D. Roberts, Rev. Mod. Phys. **82**, 2991 (2010).
  - [9] S. Kuhlmann *et al.*, Phys. Lett. B **476**, 291 (2000).
  - [10] L. T. Brady, A. Accardi, W. Melnitchouk and J. F. Owens, JHEP **1206**, 019 (2012).
  - [11] A. Accardi, M. E. Christy, C. E. Keppel, P. Monaghan, W. Melnitchouk, J. G. Morfin and J. F. Owens, Phys. Rev. D **81**, 034016 (2010).
  - [12] J. Arrington, F. Coester, R. J. Holt and T. -S. H. Lee, J. Phys. G **36**, 025005 (2009).
  - [13] J. Arrington, J. G. Rubin and W. Melnitchouk, Phys. Rev. Lett. **108**, 252001 (2012).
  - [14] A. Accardi, W. Melnitchouk, J. F. Owens, M. E. Christy, C. E. Keppel, L. Zhu and J. G. Morfin, Phys. Rev. D **84**, 014008 (2011).
  - [15] J. F. Owens, A. Accardi and W. Melnitchouk, Phys. Rev. D **87**, 094012 (2013).
  - [16] The CTEQ-Jefferson Lab (CJ) collaboration website, <http://www.jlab.org/cj>.
  - [17] L. A. Harland-Lang, A. D. Martin, P. Motylinski and R. S. Thorne, Eur. Phys. J. C **75**, 204 (2015).
  - [18] S. Dulat *et al.*, arXiv:1506.07443 [hep-ph].
  - [19] R. D. Ball *et al.*, JHEP **1504**, 040 (2015).
  - [20] F. D. Aaron *et al.*, JHEP **1001**, 109 (2010).
  - [21] V. Radescu, arXiv:1308.0374.

- [22] A. C. Benvenuti *et al.*, Phys. Lett. B **223**, 485 (1989); *ibid.* B **236**, 592 (1989).
- [23] M. Arneodo *et al.*, Nucl. Phys. B **483**, 3 (1997).
- [24] M. Arneodo *et al.*, Nucl. Phys. B **487**, 3 (1997).
- [25] L. W. Whitlow *et al.*, Phys. Lett. B **282**, 475 (1992).
- [26] S. P. Malace *et al.*, Phys. Rev. C **80**, 035207 (2009).
- [27] F. D. Aaron *et al.*, JHEP **1001**, 109 (2010).
- [28] E. A. Hawker *et al.*, Phys. Rev. Lett. **80**, 3715 (1998); J. Webb, Ph.D. Thesis, New Mexico State University (2002), arXiv:hep-ex/0301031; P. Reimer, private communication, [http://p25ext.lanl.gov/e866/papers/e866dyabs/E866\\_Drell-Yan\\_Cross\\_Sections/E866\\_Drell-Yan](http://p25ext.lanl.gov/e866/papers/e866dyabs/E866_Drell-Yan_Cross_Sections/E866_Drell-Yan)
- [29] R. S. Towell *et al.*, Phys. Rev. D **64**, 052002 (2001).
- [30] D. Acosta *et al.*, Phys. Rev. D **71**, 051104(R) (2005).
- [31] V. M. Abazov *et al.*, Phys. Rev. D **88**, 091102 (2013).
- [32] V. M. Abazov *et al.*, Phys. Rev. D **91**, 032007 (2015).
- [33] T. Aaltonen *et al.*, Phys. Rev. Lett. **102**, 181801 (2009).
- [34] V. M. Abazov *et al.*, Phys. Rev. Lett. **112**, 151803 (2014) [Phys. Rev. Lett. **114**, 049901 (2015)].
- [35] T. Aaltonen *et al.*, Phys. Lett. B **692**, 232 (2010).
- [36] V. M. Abazov *et al.*, Phys. Rev. D **76**, 012003 (2007).
- [37] T. Affolder *et al.*, Phys. Rev. D **64**, 032001 (2001).
- [38] T. Aaltonen *et al.*, Phys. Rev. D **78**, 052006 (2008).
- [39] B. Abbott *et al.*, Phys. Rev. Lett. **86**, 1707 (2001).
- [40] V. M. Abazov *et al.*, Phys. Rev. Lett. **101**, 062001 (2008).  
B. Abbott *et al.*, Phys. Rev. Lett. **86**, 1707 (2001).
- [41] V. M. Abazov *et al.*, Phys. Lett. B **666**, 435 (2008).
- [42] D. Mason *et al.*, Phys. Rev. Lett. **99**, 192001 (2007).
- [43] G. Aad *et al.*, Phys. Rev. Lett. **109**, 012001 (2012).
- [44] G. Moreno *et al.*, Phys. Rev. D **43**, 2815 (1991). ...[IS THIS CORRECT REFERENCE??]...
- [45] S. Alekhin, J. Blümlein and S.-O. Moch, Phys. Rev. D **86**, 054009 (2012).
- [46] A. D. Martin, W. J. Stirling, R. S. Thorne and G. Watt, Eur. Phys. J. C **63**, 189 (2009).
- [47] P. Jimenez-Delgado and E. Reya, Phys. Rev. D **89**, 074049 (2014).
- [48] P. Jimenez-Delgado, W. Melnitchouk and J. F. Owens, J. Phys. G: Nucl. Part. Phys. **40**,

093102 (2013).

- [49] J. Beringer *et al.* [Particle Data Group Collaboration], Phys. Rev. D **86**, 010001 (2012), <http://pdg.lbl.gov>.
- [50] H. Georgi and H. D. Politzer, Phys. Rev. D **14**, 1829 (1976).
- [51] R. K. Ellis, R. Petronzio and G. Parisi, Phys. Lett. B **64**, 97 (1976).
- [52] A. Accardi and J.-W. Qiu, JHEP **0807**, 090 (2008).
- [53] A. Accardi, T. Hobbs and W. Melnitchouk, JHEP **0911**, 084 (2009).
- [54] I. Schienbein *et al.*, J. Phys. G **35**, 053101 (2008).
- [55] L. T. Brady, A. Accardi, T. J. Hobbs and W. Melnitchouk, Phys. Rev. D **84**, 074008 (2011) [Erratum-ibid. D **85**, 039902 (2012)].
- [56] F. M. Steffens and W. Melnitchouk, Phys. Rev. C **73**, 055202 (2006).
- [57] F. M. Steffens, M. D. Brown, W. Melnitchouk and S. Sanches, Phys. Rev. C **86**, 065208 (2012).
- [58] A. De Rújula, H. Georgi and H. D. Politzer, Phys. Rev. D **15**, 2495 (1977).
- [59] A. De Rújula, H. Georgi and H. D. Politzer, Ann. Phys. **103**, 315 (1977).
- [60] M. Virchaux and A. Milsztajn, Phys. Lett. B **274**, 221 (1992).
- [61] S. I. Alekhin, S. A. Kulagin and S. Liuti, Phys. Rev. D **69**, 114009 (2004).
- [62] J. Blümlein and H. Böttcher, Phys. Lett. B **662**, 336 (2008).
- [63] J. Blümlein, Prog. Part. Nucl. Phys. **69**, 28 (2013).
- [64] W. Melnitchouk, A. W. Schreiber and A. W. Thomas, Phys. Rev. D **49**, 1183 (1994).
- [65] S. A. Kulagin, G. Piller and W. Weise, Phys. Rev. C **50**, 1154 (1994).
- [66] S. A. Kulagin and R. Petti, Nucl. Phys. A **765**, 126 (2006).
- [67] Y. Kahn, W. Melnitchouk and S. A. Kulagin, Phys. Rev. C **79**, 035205 (2009).
- [68] P. J. Ehlers, A. Accardi, L. T. Brady and W. Melnitchouk, Phys. Rev. D **90**, 014010 (2014).
- [69] R. B. Wiringa, V. G. J. Stoks and R. Schiavilla, Phys. Rev. C **51**, 38 (1995).
- [70] R. Machleidt, Phys. Rev. C **63**, 024001 (2001).
- [71] F. Gross and A. Stadler, Phys. Rev. C **78**, 014005 (2008); *ibid.* C **82**, 034004 (2010).
- [72] F. Gross and S. Liuti, Phys. Rev. C **45**, 1374 (1992).
- [73] W. Melnitchouk, A. W. Schreiber and A. W. Thomas, Phys. Lett. B **335**, 11 (1994).
- [74] J. Pumplin *et al.*, JHEP **0207**, 012 (2003).
- [75] The CTEQ collaboration website, <http://www.cteq.org>.
- [76] A. D. Martin, A. J. Th. M. Mathijssen, W. J. Stirling, R. S. Thorne, B. J. A. Watt and

- G. Watt, Eur. Phys. J. C **73**, 2318 (2013).
- [77] A. Accardi, AIP Conf. Proc. **1369**, 210 (2011).
- [78] D. Stump *et al.*, JHEP **0310**, 046 (2003).
- [79] J. Anderson [LHCb Collaboration], arXiv:1109.3371 [hep-ex].
- [80] D. d’Enterria and J. Rojo, Nucl. Phys. **B860**, 311 (2012), arXiv:1202.1762[hep-ph].
- [81] Y. Liang *et al.* [Jefferson Lab Hall C E94-110 Collaboration], arXiv:nucl-ex/0410027.
- [82] P. Monaghan, A. Accardi, M. E. Christy, C. E. Keppel, W. Melnitchouk and L. Zhu, Phys. Rev. Lett. **110**, 152002 (2013).
- [83] N. Baillie *et al.*, Phys. Rev. Lett. **108**, 142001 (2012); S. Tkachenko *et al.*, Phys. Rev. C **89**, 045206 (2014).
- [84] Jefferson Lab Experiment C12-10-103 [MARATHON], G. G. Petratos, J. Gomez, R. J. Holt and R. D. Ransome, spokespersons.
- [85] Jefferson Lab Experiment E12-10-102 [BONUS12], S. Bültmann, M. E. Christy, H. Fenker, K. Griffioen, C. E. Keppel, S. Kuhn and W. Melnitchouk, spokespersons.
- [86] Jefferson Lab Experiment E12-10-007 [SoLID], P. Souder, spokesperson.



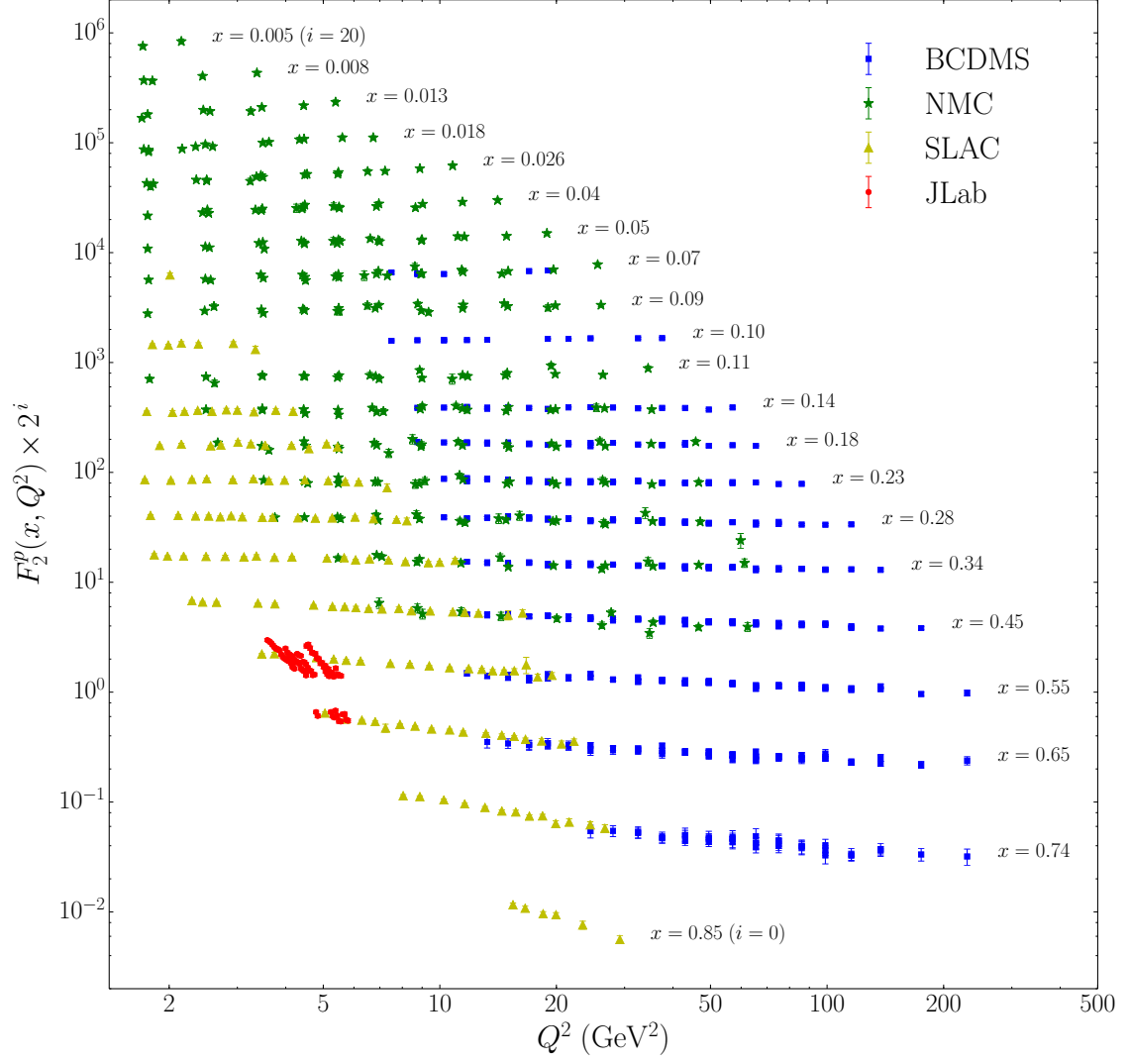


FIG. 1: Comparison of proton  $F_2^p$  structure function data used in this analysis with the CJ15 fit.

TABLE II: Parameter values for the CJ15 PDF sets at the initial scale  $Q_0 = 1.3$  GeV. The parameters without errors have been fixed.

Parameter	CJ15 value
$a_0^{uv}$	2.3585
$a_1^{uv}$	$0.60985 \pm 0.020299$
$a_2^{uv}$	$3.5377 \pm 0.011405$
$a_3^{uv}$	0
$a_4^{uv}$	$3.5169 \pm 0.42791$
$a_5^{uv}$	0
$a_0^{dv}$	23.233
$a_1^{dv}$	$1.1387 \pm 0.034586$
$a_2^{dv}$	$6.6180 \pm 0.15977$
$a_3^{dv}$	$-3.5743 \pm 0.090782$
$a_4^{dv}$	$4.9133 \pm 0.14586$
$a_5^{dv}$	0
$a_6^{dv}$	$-0.0042424 \pm 0.00070691$
$a_7^{dv}$	2
$a_0^{\bar{u}+\bar{d}}$	$0.14121 \pm 0.0050459$
$a_1^{\bar{u}+\bar{d}}$	$-0.21785 \pm 0.0039454$
$a_2^{\bar{u}+\bar{d}}$	$8.4003 \pm 0.14833$
$a_3^{\bar{u}+\bar{d}}$	0
$a_4^{\bar{u}+\bar{d}}$	$16.055 \pm 1.1403$
$a_5^{\bar{u}+\bar{d}}$	0
$a_0^{\bar{d}-\bar{u}}$	35712
$a_1^{\bar{d}-\bar{u}}$	$3.9867 \pm 0.049301$
$a_2^{\bar{d}-\bar{u}}$	$20.289 \pm 0.66322$
$a_3^{\bar{d}-\bar{u}}$	17
$a_4^{\bar{d}-\bar{u}}$	$49.881 \pm 7.1398$
$a_0^g$	46.706
$a_1^g$	$0.61586 \pm 0.038277$
$a_2^g$	$6.2335 \pm 1.1222$
$a_3^g$	$-3.2703 \pm 0.16746$
$a_4^g$	$3.0338 \pm 0.31300$
$a_5^g$	0
$\kappa$	0.4
$C_0$	$0.098222 \pm 0.028518$
$x_0$	$0.34487 \pm 0.91982$
$x_1$	0.048
$h_1$	$-3.0094 \pm 0.24080$
$h_2$	$1.7526 \pm 0.10135$
$h_3$	$-2.0895 \pm 0.026853$
$\Lambda_{\text{QCD}}^{(4)}$	0.2268 GeV
$m_c$	1.3 GeV
$m_b$	4.5 GeV

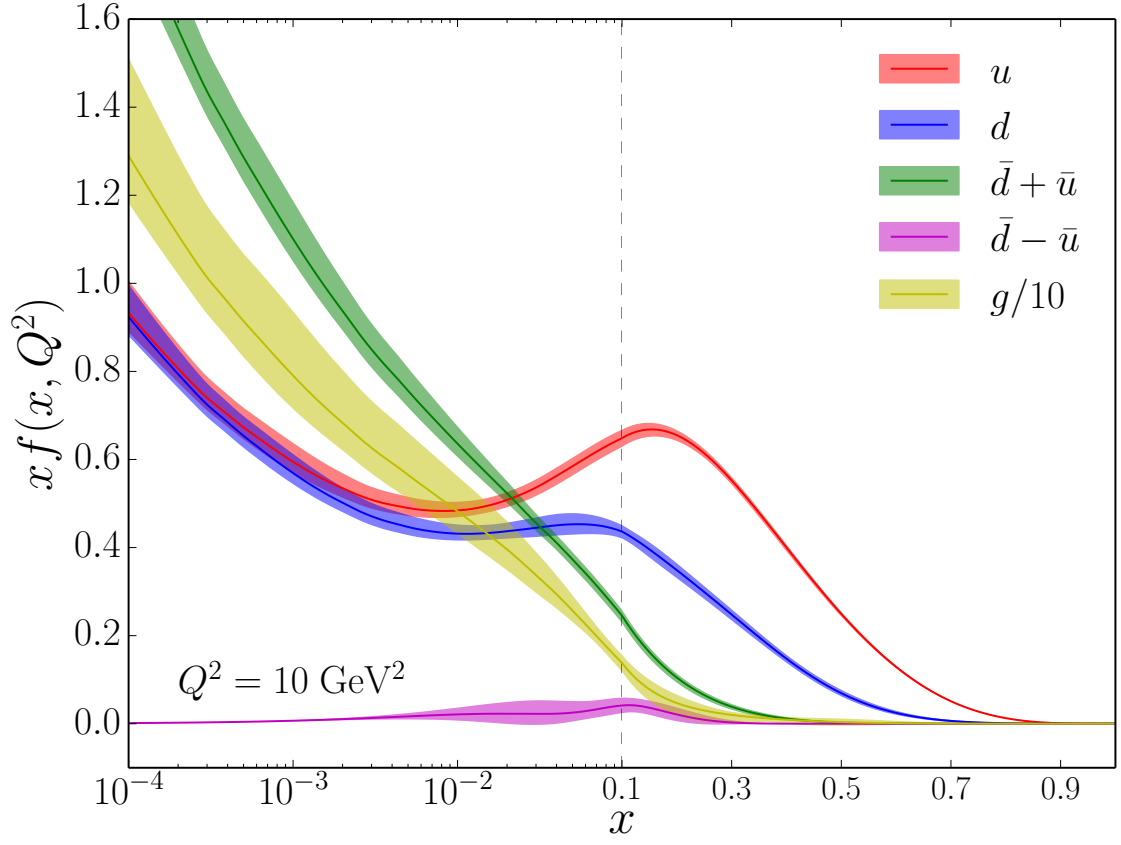


FIG. 2: Comparison of CJ15 PDFs for different flavors ( $u, d, \bar{d} + \bar{u}, \bar{d} - \bar{u}$  and  $g/10$ ) at a scale  $Q^2 = 10 \text{ GeV}^2$ . Note the combined logarithim/linear scale along the  $x$ -axis.

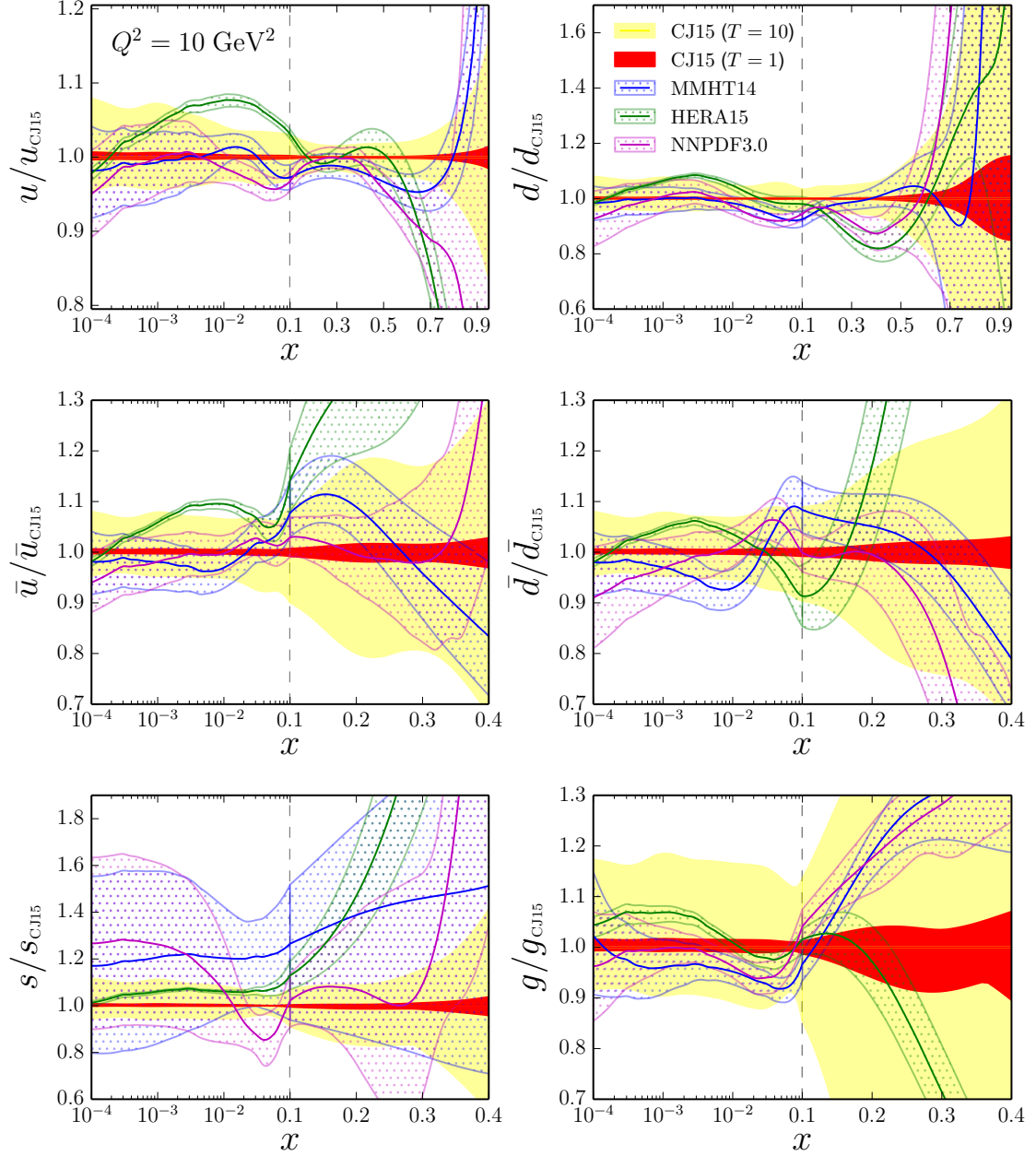


FIG. 3: Ratio of PDFs to the CJ15 central values for various PDF sets: CJ15 for tolerance  $T = 1$  (red) and  $T = 10$  (yellow), MMHT14 [17] (blue), HERA15 [21] (green), and NNPDF3.0 [19] (magenta). Note the different scales on the vertical axes used for different flavors.

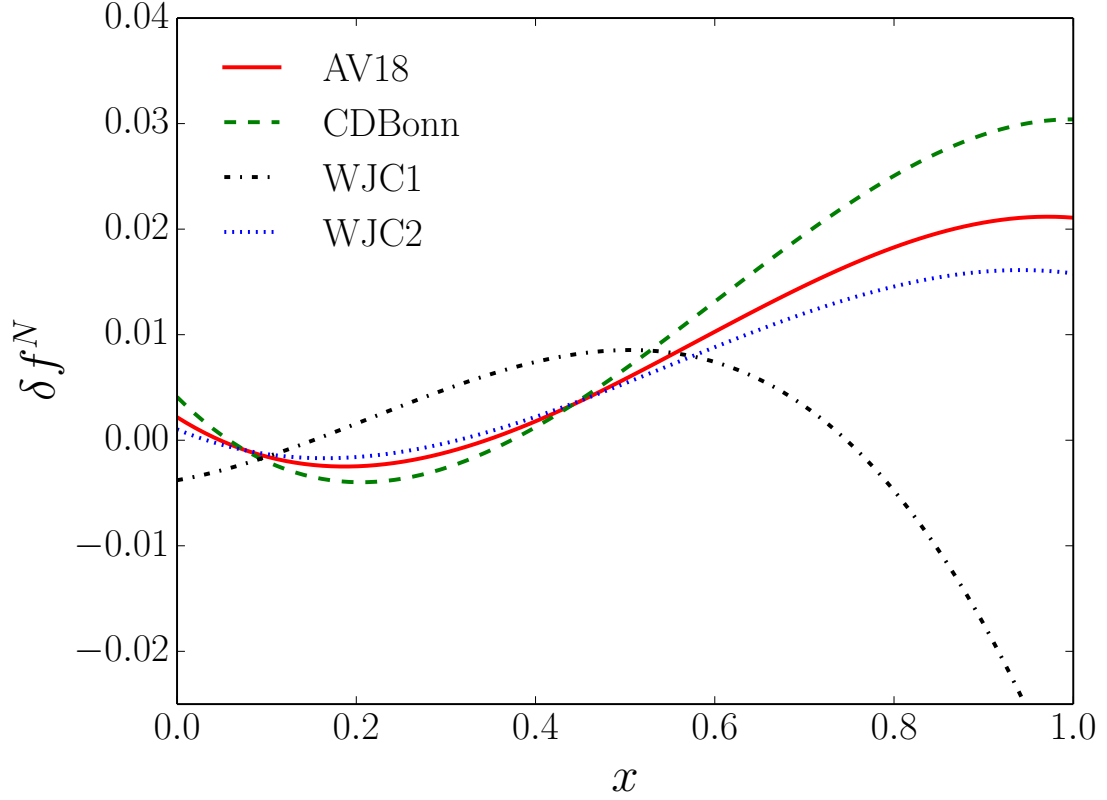


FIG. 4: Fitted nucleon off-shell correction  $\delta f^N$  for the parametrization in Eq. (10), using the AV18 (solid line), CD-Bonn (dashed line), WJC-1 (dot-dashed line) and WJC-2 (dotted line) wave functions.

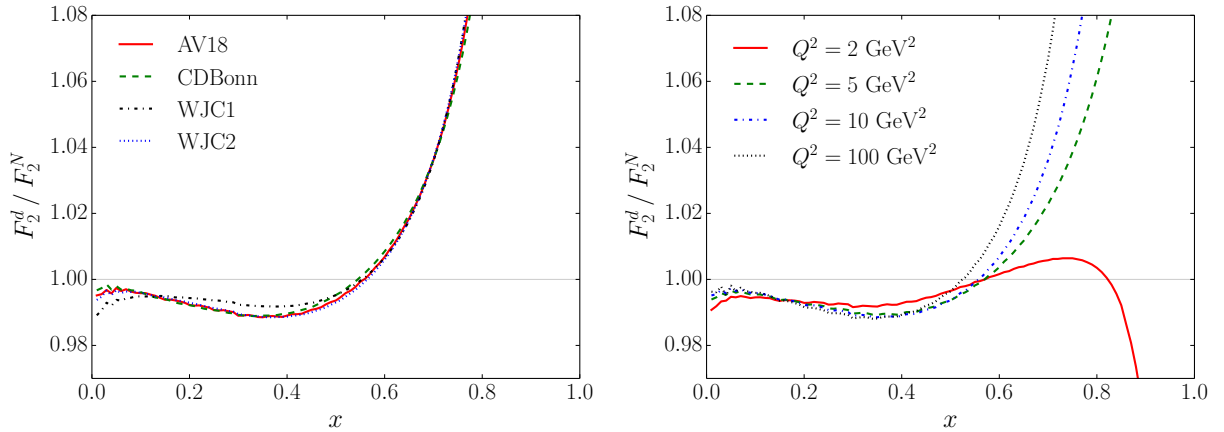


FIG. 5: Ratio of deuteron to isoscalar nucleon structure functions  $F_2^d/F_2^N$  for **(a)** different deuteron wave function models at  $Q^2 = 10 \text{ GeV}^2$ , and **(b)** different values of  $Q^2$  for the AV18 wave function.

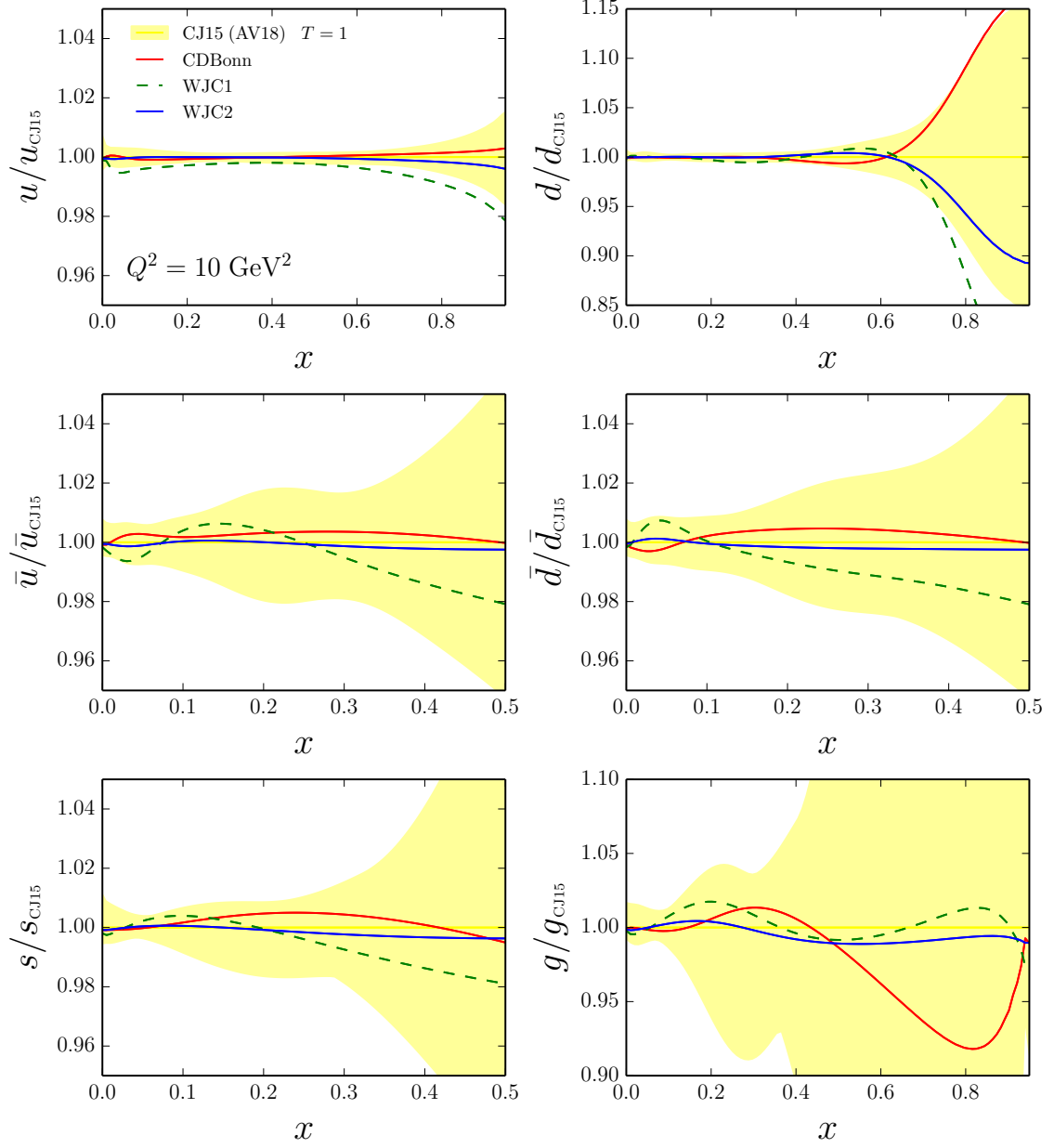


FIG. 6: Ratio of CJ15 PDFs (with  $T = 1$ ) for various deuteron wave function models: AV18 (yellow band), CD-Bonn (red solid lines), WJC-1 (green dashed lines), WJC-2 (blue solid lines), for the off-shell parametrization (10). The PDF ratios are taken with respect to those for the AV18 wave function. Note the different scale on the vertical axes for the  $d$ -quark and gluon distributions.

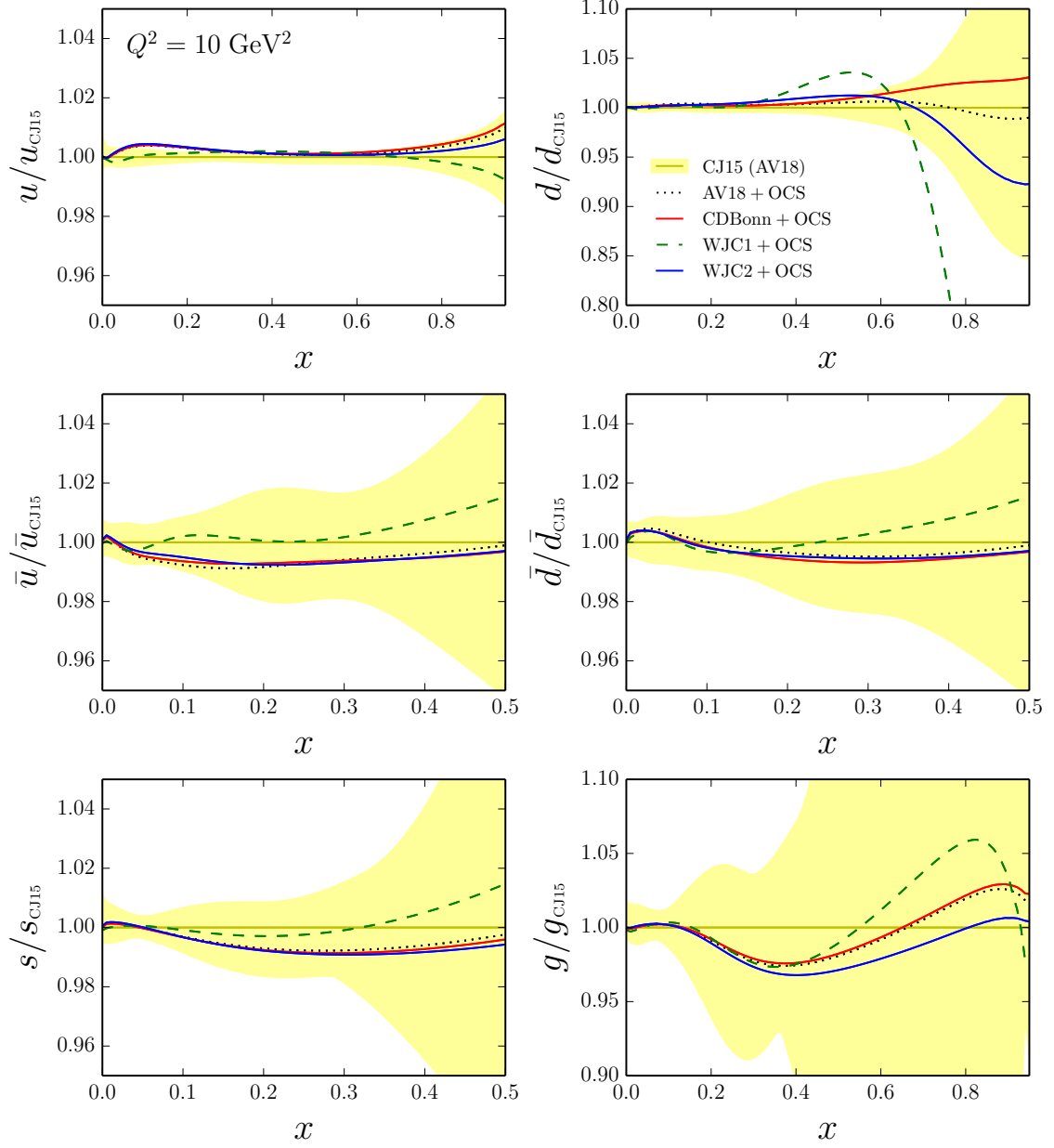


FIG. 7: Ratio of PDFs for the off-shell covariant spectator (OCS) model with different deuteron wave functions to the CJ15 PDFs (which uses the off-shell parametrization (10) and the AV18 deuteron wave function): OCS model with AV18 (black dotted lines), CD-Bonn (red solid lines), WJC-1 (green dashed lines), and WJC-2 (blue solid lines). Note the different scale on the vertical axes for the  $d$ -quark and gluon distributions.

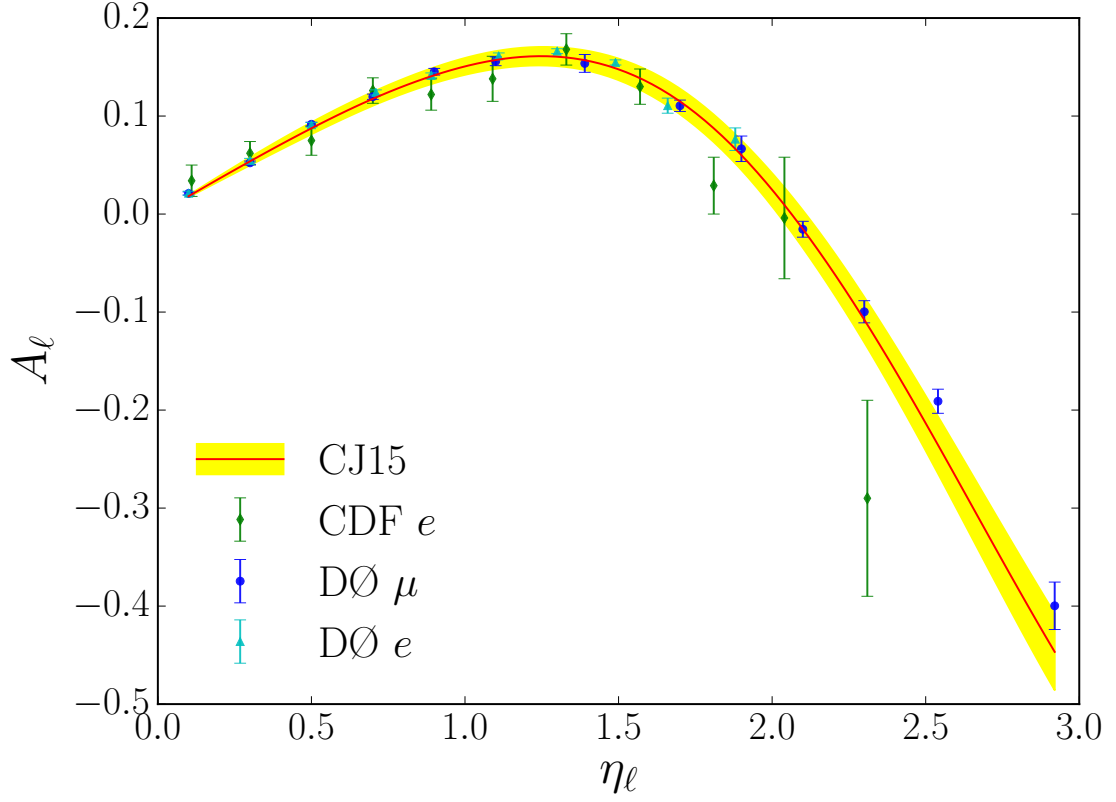


FIG. 8: Lepton charge asymmetry  $A_\ell$  from  $p\bar{p} \rightarrow WX \rightarrow \ell\nu X$  as a function of the lepton pseudo-rapidity  $\eta_\ell$  from CDF electron (diamonds) [30] and DØ muon (circles) [31] and electron (triangles) [32] data compared with the CJ15 fit.



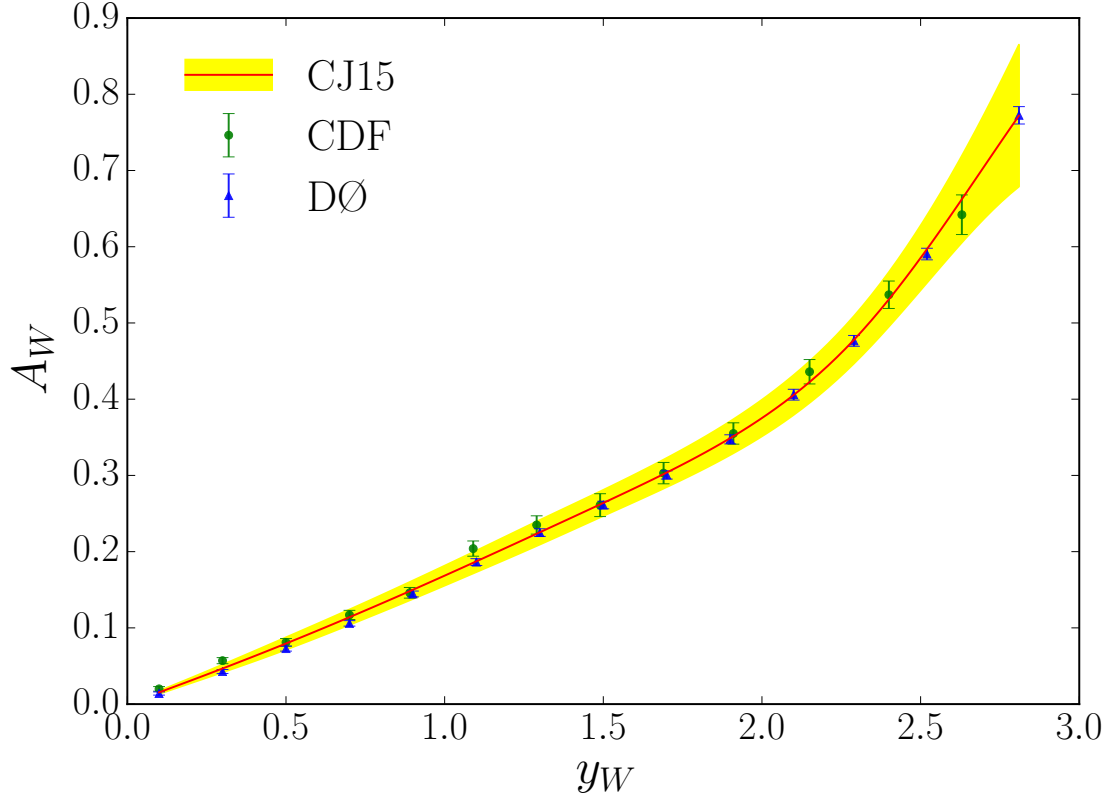


FIG. 9:  $W$  boson charge asymmetry  $A_W$  from  $p\bar{p} \rightarrow WX$  as a function of the  $W$  boson rapidity  $y_W$  for CDF (circles) [33] and DØ (triangles) [34] data compared with the CJ15 fit.

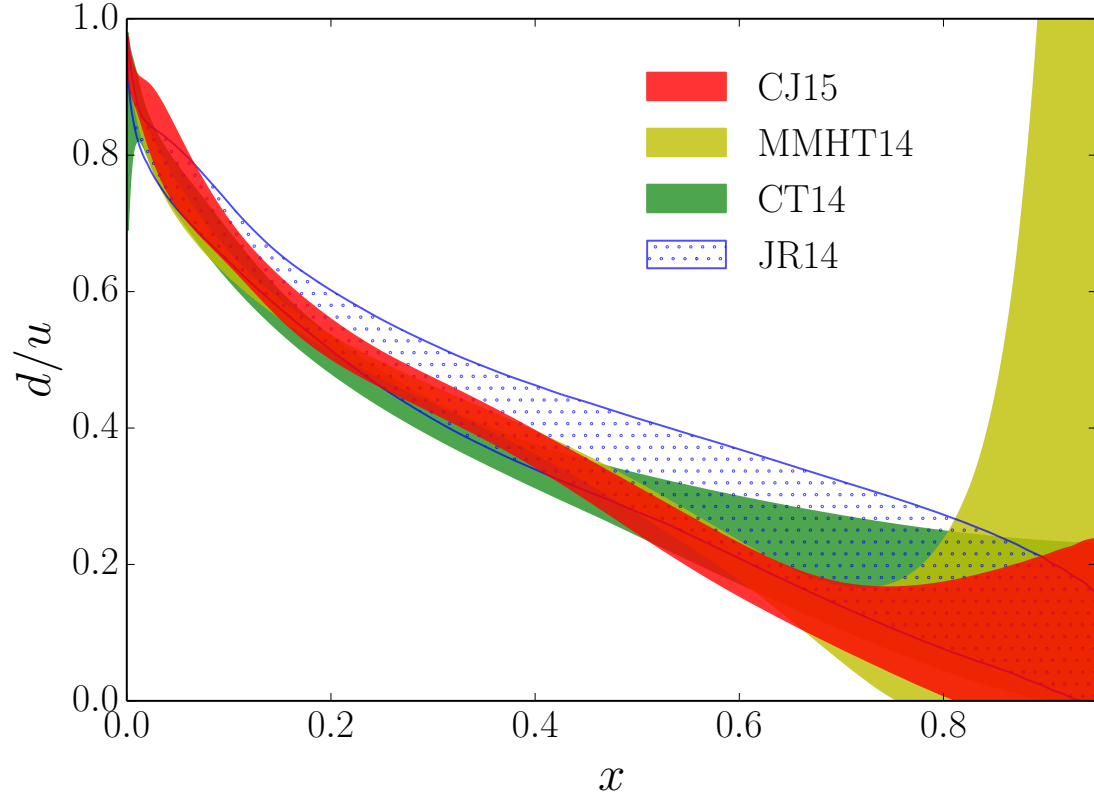


FIG. 10: Comparison of the  $d/u$  ratio at  $Q^2 = 10 \text{ GeV}^2$  for different PDF parametrizations: CJ15 (red band), MMHT14 [17] (yellow band), CT14 [18] (green band), and JR14 [47] (blue dotted band).

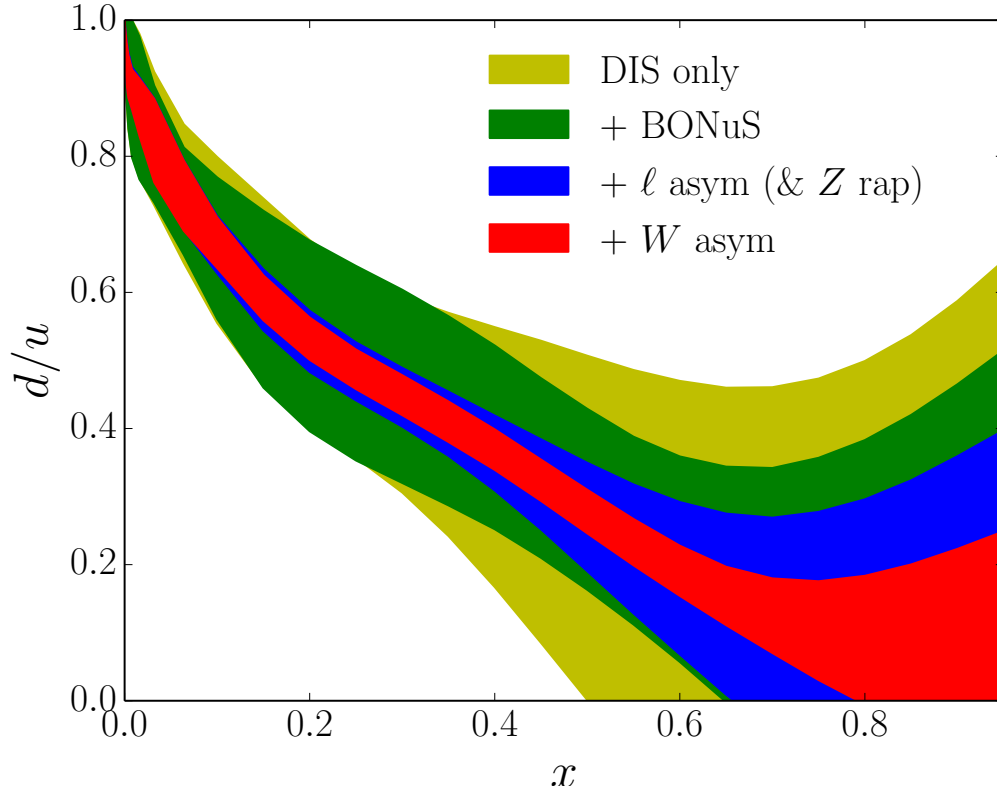


FIG. 11: Impact of various data sets on the  $d/u$  ratio at  $Q^2 = 10 \text{ GeV}^2$ . The uncertainty band is largest for the DIS only data (yellow band), and decreases with the successive addition of Jefferson Lab  $F_2^n/F_2^d$  BONuS [83] data (green band), lepton asymmetry [30–32] (and  $Z$  rapidity [35, 36]) data (blue band), and  $W$  boson asymmetry data [33, 34] (red band).

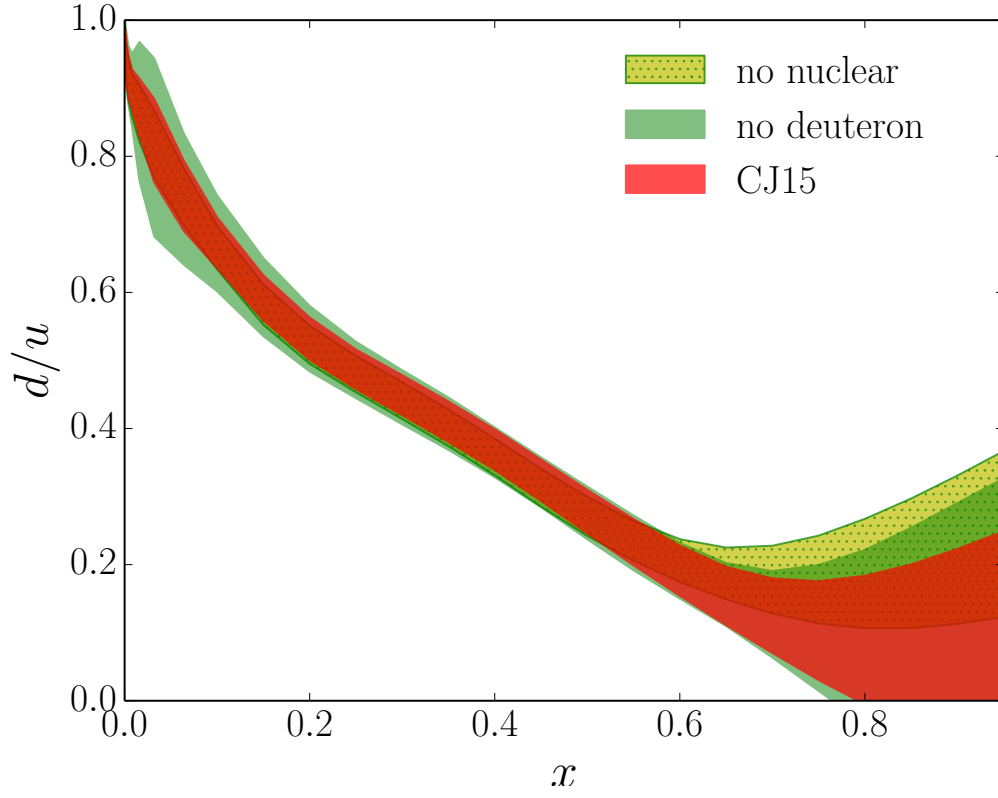


FIG. 12: Impact on the full CJ15 fit (red band) of removing the deuteron nuclear corrections (yellow hatched band), and omitting the deuteron data (green band).